Construction and Building Materials 68 (2014) 740–749

Contents lists available at ScienceDirect

Construction and Building Materials

journal homepage: www.elsevier.com/locate/conbuildmat

Effect of styrene–butadiene copolymer latex on properties and durability of road base stabilized with Portland cement additive

Mojtaba Shojaei Baghini [a,b], Amiruddin Ismail [a,b,*], Mohamed Rehan Karim [c], Foad Shokri [a,b], Ali Asghar Firoozi [b]

[a] Sustainable Urban Transport Research Centre (SUTRA), Universiti Kebangsaan Malaysia, Malaysia
[b] Department of Civil and Structural Engineering, Universiti Kebangsaan Malaysia, Malaysia
[c] Department of Civil Engineering, Faculty of Engineering, University of Malaya, Malaysia

HIGHLIGHTS

- Cement additive and styrene–butadiene emulsion (Tylac® 4190) mixes investigated.
- Additive has improved the strength of mixes.
- WD tests on 4% Portland cement and 8% Tylac® 4190 mix reduce 86.99% water absorption.
- We develop nonlinear models to predict strength based on mixture parameters.

ARTICLE INFO

Article history:
Received 19 February 2014
Received in revised form 9 May 2014
Accepted 29 June 2014

Keywords:
Cement-treated base
Unconfined compressive strength
Indirect tensile strength
Indirect tensile resilient modulus
Wetting
Drying
Durability
Regression analysis

ABSTRACT

This study investigated the effects of the type and amount of Portland cement and carboxylated styrene–butadiene emulsion (Tylac® 4190) on the short-term performance of a road base layer via a laboratory evaluation of stabilized soil-aggregate mixtures. Cylindrical specimens stabilized with Portland cement (0–6%), Tylac® 4190 (5–10%), and a mixture of both these additives were molded, cured for 7, 28, and 60 days, and then subjected to different stress sequences to study the unconfined compressive strength, indirect tensile strength, and indirect tensile resilient modulus. The long-term performance (durability) of stabilized soil-aggregate specimens was investigated by conducting wetting and drying (WD) cycling tests on 7-day-cured soil-aggregate specimens stabilized with cement and Tylac® 4190. The results revealed that the additives improved the strength of the specimens, which has been found to be an important quality indicator of road base mechanical properties. Results of tests conducted to assess the specimens' resistance to WD cycling showed that the addition of a 4% Portland cement–8% Tylac® 4190 mixture resulted in reductions of 86.99% in both water absorption and permeability, volume changes of 88.55%, and weight changes of 92.84% relative to a sample with only 4% cement after 12 WD cycles. This paper also presents the findings of a correlation study conducted for determining the influences of affective variables using nonlinear regression analysis to establish significant prediction models for strength based on mixture parameters.

1. Introduction

Factors such as an increased number of vehicles, traffic loading, and tire pressure have motivated pavement engineers to develop better technologies for increasing the pavement bearing capacity and improving short-term and long-term pavement performances. A variety of soils or granular materials are available for the construction of road bases, but they may exhibit inadequate properties, e.g., low bearing capacity, susceptibility to moisture damage, and susceptibility to environmental conditions, which would in turn result in substantial pavement distress and shortening of pavement life. However, the addition of a stabilizing agent can improve the properties of a soil-aggregate mixture. Soil-aggregate stabilizers are categorized as either traditional or nontraditional. Traditional additives include cement, lime, fly ash, and bituminous materials, whereas nontraditional additives include enzymes,

* Corresponding author at: Head, Sustainable Urban Transport Research Centre (SUTRA), Universiti Kebangsaan Malaysia, Malaysia.
E-mail addresses: msbaghini@yahoo.com (M. Shojaei Baghini), abim@eng.ukm.my (A. Ismail), rehan@um.edu.my (M.R. Karim), foad_shokri@yahoo.com (F. Shokri), mehran.firoozi@gmail.com (A.A. Firoozi).

http://dx.doi.org/10.1016/j.conbuildmat.2014.06.061
0950-0618/

liquid polymers, resins, acids, silicates, ions, and lignin derivatives. Among these different stabilizing materials, cement-treated base (CTB) develops significantly high stiffness and strength and exhibits good serviceability and high durability when used for pavement construction. Cement stabilization of soil was initiated on a trial basis in 1917, and since then, several works have been published on this topic [1–6]. Polymer stabilizers are typically vinyl acetates or acrylic copolymers suspended in an emulsion by surfactants. The polymer stabilizer coats soil-aggregate particles, and physical bonds are formed when the emulsion water evaporates, leaving a soil–polymer matrix. The emulsifying agent can also serve as a surfactant, improving penetration for topical applications and particle coating under admix conditions. The use of polymers as modifiers in new structures seems to be a promising strategy for improving the microstructure of mixtures and enhancing their durability [7–11]. Polymers have a significant effect on the workability and mechanical properties of soil aggregate–cement mixture. The literature usually refers to the more commonly used styrene–butadiene polymer materials. These materials are known to possess superior durability over ordinary Portland-cement-based concrete, and are resistant to acid attack, ice melting, and chloride diffusion. Several authors have shown that polymer impregnation of soil aggregate–cement materials may lead to increased durability depending on the type of polymers used. Previous studies have also indicated that the admixing of styrene–butadiene emulsion (SBE) latex into a mixture improved its resistance to chloride-ion penetration [10,12–16]. The molecular structure of SBE includes both flexible butadiene chains and rigid styrene chains, the combination of which lends many desirable characteristics to SBE-modified soil aggregate–cement materials, such as good mechanical properties, water tightness, and abrasion resistance [12,17–20]. A cement–SBE-treated base (CSBETB) can provide cost-effective solutions to many common designs and construction scenarios and impart additional strength and support without increasing the total thickness of the pavement layers. Depending on the requirements of a project, CSBETB can increase the construction speed and enhance the structural capacity of the pavement. In addition, a stiffer base reduces deflections due to heavy traffic loads, thereby extending pavement life [4,21–27]. CSBETB can also distribute loads over a wider area and reduce the stresses on the subgrade. It has a high load-carrying capacity, does not consolidate further under load, reduces rutting in hot-mix asphalt pavements, and is resistant to freeze–thaw and wetting–drying (WD) deterioration [28–30]. The goal of the present work was to assess the factors affecting the performance and strength of Cement–Tylac® 4190 treated base (CTTB) via laboratory tests aimed at determining its unconfined compressive strength (UCS), indirect tensile strength (ITS), and indirect tensile resilient modulus (ITRM), as well as WD cycling tests, which are the most frequently employed factors for assessing the degree of road base stabilization (RBS). Another goal was to determine the optimum contents of Portland cement and Tylac® 4190 in their mixture. The last but most important goal of the work was to compare the effects of these two additives on the soil-aggregate mixtures using significant prediction models.

2. Standard requirements for use of graded soil-aggregate in bases of highways

Quality-controlled graded aggregates are expected to provide appropriate stability and load support for use as highway or airport bases or sub-bases. This requirement delineates the aggregate size, variety, and ranges of mechanical analysis results for standard sizes of coarse aggregate and screenings of aggregates for their use in the construction and maintenance of various types of highways. The gradation of the final composite mixture is required to conform to an approved job mix formula within the design range prescribed in Table 1 in accordance with ASTM D 448, ASTM D 1241, and ASTM D 2940, subject to the appropriate tolerances.

3. Strength requirements for stabilized road base material

After obtaining the fitting aggregates and choosing the initial cement content by weight, the specimens were prepared according to their optimum dry density and the maximum moisture composition. The average UCS of the cement-treated specimens cured for 7 days was measured using a hydraulic compressive strength testing machine to detect the optimum content of cement. Table 2 lists the UCS requirements of CTB subjected to curing for 7 days. It should be noted that the UCS requirements depend strongly on the road class, and the material type relies heavily on the required UCS.

4. Materials and methods

To achieve the goals of this study, three major tasks—a literature review, laboratory investigation, and data processing and analyses—were accomplished. The soil-aggregate properties were evaluated prior to the design of the mixture, and those physical properties namely index test. The cement used was type II Portland cement. The nontraditional stabilizer used, Tylac® 4190, is a water-based liquid emulsion and is a novel additive in this method. To evaluate the short-term performance of the stabilized soil-aggregate specimens under various stress sequences, the UCS, ITS, and ITRM were determined. The long-term performance of these specimens was investigated by subjecting them to repeated WD cycles. Finally, on the basis of the results of data analysis, significant models were developed to demonstrate the relationship among the characteristics of the mixture.

4.1. Aggregates

Crushed granite aggregates from the Kajang Rock Quarry (Malaysia) were used as the granular base layer material in this study. Fig. 1 illustrates the grading curves of soil-aggregates within the limits specified by the ASTM standards for highways and/or airports. One of the most important factors affecting the performance of CTB is its organic content. In all probability, a soil with an organic content greater than 2% or having a pH lower than 5.3 will not react normally with cement [32]. A pH greater than 12.0 for a mixture indicates that the organics present will not interfere with hardening [33,34]. In this study, the results of a pH test conducted according to ASTM D 4972 indicated that adding cement to the soil-aggregate increases the pH from 8.26 to 12.13 whereas adding a cement–Tylac® 4190 mixture to the soil-aggregate increases the pH from 8.26 to 12.39. This clearly shows that the additives have a positive effect in the mixture.

The general properties of the used soil-aggregates are summarized in Table 3. Table 3 lists the most correlated geotechnical properties of the soil-aggregates used in this study.

4.2. Portland cement

Various kinds of Portland cement have been used effectively for soil-aggregate stabilization. In this study, type II Portland cement was used as a treatment material for the granular mixtures because of its higher sulfate resistance, moderate heat of hydration, and mostly equivalent cost in comparison to other types of Portland cement. A high sulfate content of soil results in swell and heave problems, and it can have a deleterious influence on cementing and stabilization mechanisms. The Portland cement used in this study was required to conform to the respective standard chemical and physical requirements prescribed by ASTM C 150 and ASTM C 114. The cement would be rejected if it does not meet any of the necessary specifications. The properties of type II Portland cement are presented in Table 4.

4.3. Water

The mixing water used for these tests should be free of acids, alkalis, and oils, and in general, it should be suitable for drinking, according to ASTM D 1632 and ASTM D 4972. According to ASTD D1193, water is classified into four grades-types I, type II, type III, and type IV-depending on its physical, chemical, and biological properties. All the mixed water used for these test methods should be ASTM type III or better. Water prepared by distillation is of type III.

4.4. Tylac® 4190

Tylac® 4190 is proposed as a polymer modifier for hydraulic cement mixtures or tile mortar adhesives. It is surfactant-stabilized styrene–butadiene copolymer latex used in concrete, mortar, grout, and cement mixtures; when used properly (mixed

Table 1
Grading requirements for final mixtures [31].

Sieve size (square openings)	Design range (mass percentages passing)		Job mix tolerances	
	Bases	Sub-bases	Bases	Sub-bases
50 mm (2 in.)	100	100	−2	−3
37.5 mm (1 1/2 in.)	95–100	90–100	±5	+5
19.0 mm (3/4 in.)	70–92	NA	±8	NA
9.5 mm (3/8 in.)	50–70	NA	±8	NA
4.75 mm (No. 4)	35–55	30–60	±8	±10
600 μm (No. 30)	12–25	NA	±5	NA
75 μm (No. 200)	0–8	0–12	±3	±5

Table 2
Strength requirements for CTB.

Country	Other research	Compressive strength (psi)	Cement content (%)	Refs.
	CTB	300–600		[2–4]
	CTB	750		[4,5]
	CTB	300–800		[6]
	CTB	435–870		[7,8]
	CTB	Min–500		[9]
South Africa		580–1160		[7,10]
United Kingdom		363–653		[11,12]
Australia		Min–435		[13,14]
China		435–725		[14,15]
New Zealand		Min–435		[16]
		Min–600		[17]
United States (ASTM)			3–5	[1,12,18]
United States (AASHTO)			3–5	[12,18,19]

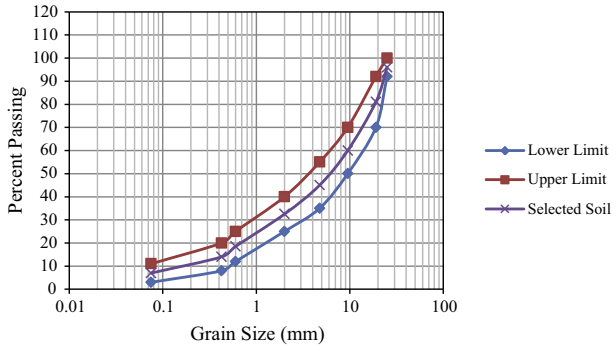

Fig. 1. Grading curves for soil-aggregate.

well before and after use), it can produce mixtures that exhibit improved adhesion to most substrates, improved water resistance, increased flexural strength, increased resistance to freezing and thawing, and reduced water/cement ratios. The properties of Tylac® 4190 are presented in Table 5.

5. Results and discussion

5.1. Moisture content–dry density relationship of the mixtures

The dry density of compacted soil-aggregate is one of the main factors influencing the strength of CTB. In addition, water is essential for achieving maximum density and for promoting the hydration of cement. Method C of ASTM D 698 is a laboratory compaction method used to determine the relationship between the water content and the dry unit weight of soil-aggregates compacted in a 152.4-mm-diameter mold with a 24.4-N rammer dropped from a height of 305 mm, producing a compactive effort of 600 KN-m/m^3. This method was used in the present study. Specifically, three layers of a soil-aggregate at selected water content were placed in the mold of given dimensions, where each layer was compacted by 56 blows of the rammer. Further, according to ASTM D 558 Method B, the relationship between the water content and the dry density of the soil aggregate–cement mixtures was determined using a cylindrical metal mold having a capacity of 944 cm^3 and internal diameter of 101.60 mm. The mixtures were compacted using a 2.49 kg metal rammer having a 50.80 mm diameter dropped from a height of 305 mm. To prepare the specimens, the required amount of cement was added to the soil-aggregate in conformance to specifications ASTM C 150 and C 595, and the resulting mixture was mixed thoroughly to achieve a uniform color. Water was then added to this soil aggregate–cement mixture and specimens were prepared by compacting this mixture in the mold in three equal layers, where each layer was compacted by 25 blows to give a total compacted depth of about 130 mm. This exact process was also applied for mixing cement with Tylac® 4190. Fig. 2 shows the compaction curves that demonstrate the relationship between the dry density and moisture content at various cement contents, as obtained for non-stabilized soil-aggregate according to ASTM D 698 and for a CTB mixture prepared with different cement contents, according to ASTM D 558.

Fig. 2 shows that both the optimum water content and the maximum dry density increase with an increase in the cement content when the compaction moisture is increased by about 0.25% for each 1.0% increase in the cement added to the specimen. This can be explained using the theoretical formulation of the overall void ratio of the mixture comprising soils with varying grain sizes. Lade et al. [35] showed that when small particles are added to a large-sized particle matrix, the overall void ratio decreases until all the voids are filled with small particles. This means that the dry density increases up to a specific mixing ratio of small and large particles. In addition, according to ASTM D 558, the maximum dry density of the cement–Tylac® 4190 mixture is obtained at a cement content of 4% and Tylac® 4190 content of 5–10%, and this parameter can be used as an important variable for predicting models. The plot of the maximum dry density vs. the content of Tylac® 4190 in the cement–Tylac® 4190 mixture is shown in Fig. 3.

Specifically, based on experimental data, the linear model in Fig. 3 shows the relationship between the content of Tylac® 4190 in the cement–Tylac® 4190 mixture and the maximum dry density as obtained for the CTTB mixture according to ASTM D 558. It is seen that the maximum dry density increases with an increase in the Tylac® 4190 content up to 8%. This trend can be explained by the consolidation of both the rigid styrene chains and the flexible butadiene chains of the SBE molecular structure, which enhances the mechanical properties of the mixture. Tylac® 4190 has very small particles (nanosized), so it spreads and penetrates throughout the soil aggregate–cement structure to provide toughness and flexibility to it. However, after that, the maximum dry density decreases with an increase in the Tylac® 4190 content on account of the higher water content of 44.92% of Tylac® 4190; this leads to a decrease in the strength of the mixture. The presence of too much water in the mixture poses a problem because it inhibits adequate compaction and decreases the toughness and flexibility of the soil aggregate–cement structure, resulting in a decrease in the dry unit weight.

5.2. UCS

The primary purpose of the UCS test is to determine the approximate compressive strength of a mixture that has sufficient cohesion to permit testing in the unconfined state. For this test, the mixture was prepared according to ASTM D 1632 using a metal cylinder with an internal diameter of 101.60 mm and height of

Table 3
Properties of soil-aggregates used in this study.

Property	Requirements	Test result	Test method
Water content (%)	NA	6.621	ASTM D 698
Unit weight (g/cm^3)	NA	2.19	ASTM D 698
pH	5.3–Min	8.26	ASTM D 4972
Unified classification	NA	GP-GM	ASTM D 2487
AASHTO classification	NA	A-1-a	ASTM D 3282/AASHTO M 145
Liquid limit (%)	25–Max	21.4	ASTM D 4318
Plastic limit (%)	29–Max	19.6	ASTM D 4318
Plastic index (%)	4–Max	1.8	ASTM D 4318
Coefficient of curvature (Cc)	NA	2.39	ASTM D 2487
Coefficient of uniformity (Cu)	NA	71.5	ASTM D 2487
Group index	NA	0	ASTM D 3282
Specific gravity (OD)	NA	2.659	ASTM C 127/C 128
Specific gravity (SSD)	NA	2.686	ASTM C 127/C 128
Apparent specific gravity	NA	2.731	ASTM C 127/C 128
Water absorption (%)	2–Max	0.973	ASTM C 127/C 128
Linear shrinkage (%)	3–Max	1.5	BS 1377: Part 2
Elongation index (%)	25–Max	13.03	BS 812: Section 105.2
Flakiness index (%)	25–Max	7.68	BS 812: Section 105.1
Average least dimension (mm)	NA	5.5	BS 812: Section 105.1
Sand equivalent (%)	35–Min	84	ASTM D 2419
Los Angeles abrasion (%)	50–Max	17.5	ASTM C131
UCS (MPa)	NA	0.25	ASTM D 2166/D 1633
CBR (%)	80–Min	101.32	ASTM D 1883

Table 4
Properties of type II Portland cement.

Properties	Requirements (%)	Test result (%)	Test method
Silicon dioxide (SiO_2)	20-Min	20.18	ASTM C 150-C 114
Aluminum oxide (Al_2O_3)	6.0-Max	5.23	ASTM C 150-C 114
Calcium oxide (CaO)	Not applicable	64.40	ASTM C 150-C 114
Ferric oxide (Fe_2O_3)	6.0-Max	3.34	ASTM C 150-C 114
Magnesium oxide (MgO)	6.0-Max	1.80	ASTM C 150-C 114
Sulfur trioxide (SO_3)	6.0-Max	3.03	ASTM C 150-C 114
Loss on ignition	3.0 -Max	2.17	ASTM C 150-C 114
Insoluble residue	0.75-Max	0.18	ASTM C 150-C 114
Na_2O	Not applicable	0.07	ASTM C 150-C 114
K_2O	Not applicable	0.44	ASTM C 150-C 114
Equivalent alkalies ($Na_2O + 0.658K_2O$)	0.75-Max	0.3595	ASTM C 150-C 114
Tricalcium aluminate (C_3A)	8-Max	3.21	ASTM C 150-C 114
Tricalcium silicate (C_3S)	Not applicable	53.95	ASTM C 150-C 114
Sum of (C_3S) and (C_3A)	58-Max	57.16	ASTM C 150-C 114
Compressive strength, MPa:			ASTM C 109/C 109 M
3 days	10-Min	27.5	
7 days	17-Min	40.3	
28 days	28-Min	57.7	
Fineness, specific surface, m^2/kg:			ASTM C 204
Air permeability test	280-Min	338.1	
Autoclave expansion (Soundness)	0.8-Max	0.5	ASTM C 151

Table 5
Properties of Tylac® 4190.

Chemical name	Carboxylated SBE
Physical state	Liquid
Color	White, Milky
Boiling point	100 °C at 17 mmHg
Solids Content	46.0–48%
Vapor density	<1, (Air = 1)
Vapor pressure	17 mmHg @ 20 °C
Solubility in water	Miscible
pH	10.71
Specific gravity	1.00–1.03
Emulsifiers	Anionic
Viscosity (Brookfield #2/20 rpm)	200 max cps
Particle diameter	0.18 μm
Glass transition temp. (Tg)	+3 °C
Water content (% by weight)	44.92

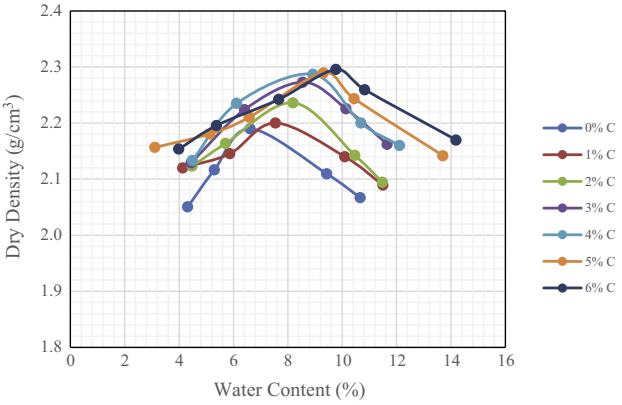

Fig. 2. Relation between moisture content and dry density at various cement contents. "C" denotes cement.

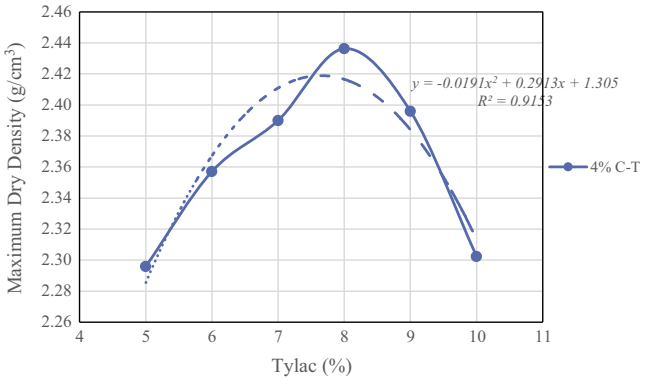

Fig. 3. Plot of maximum dry density vs. content of Tylac® 4190 in the cement–Tylac® 4190 mixture. "C" denotes cement and "T" denotes Tylac® 4190; y is the maximum dry density [g/cm^3] and x is the Tylac® 4190 content [%].

116.4 mm. The specimens were placed for 12 h in the molds in a moist room for curing; subsequently, the specimens were removed using a sample extruder. The removed specimens were wrapped in plastic for protection against dripping water for a specific duration of moist curing in the moist room. The average UCS of the specimens cured for 7, 28, and 60 days was determined using a hydraulic compressive strength testing machine by applying a load at a constant rate within the range of 140 ± 70 kPa/s according to ASTM D 1633. Finally, the unit compressive strength [MPa] was calculated by dividing the maximum load [N] by the cross-sectional area [mm^2]. The influences of the cement content, Tylac® 4190 content, and curing time on the UCS of the mixture are shown in Figs. 4–6, respectively.

Specifically, Fig. 4 shows the influence of the cement content on the UCS of the mixture for 7 days and 28 days of curing, using two linear models based on experimental data. This figure reveals a proportional relationship between these two parameters. In other words, an increase in the cement content causes an increase in the UCS of the mixture on account of the hydration products of the cement that fill the pores of the matrix and thus enhance the rigidity of its structure by forming a large number of rigid bonds in the soil-aggregate. On the basis of this graph and the strength requirements for CTB listed in Table 2, the optimum cement content was chosen as 4%.

Fig. 5 shows the influence of the Tylac® 4190 content on the UCS for 7 days and 28 days of curing. It is seen that an increase in the Tylac® 4190 content causes the UCS of the mixture to increase owing to the presence of both flexible butadiene chains and rigid styrene chains in the SBE molecular structure, the consolidation of which provides good mechanical properties such as increased strength, water tightness, and abrasion resistance up to

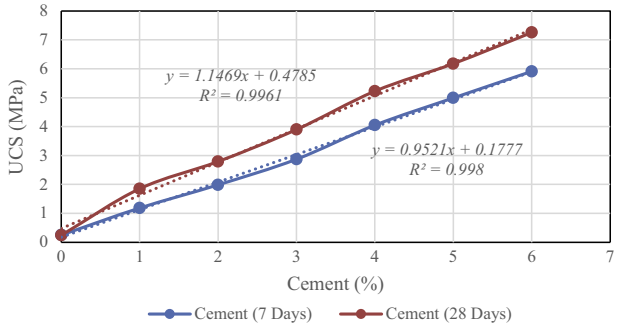

Fig. 4. Plot of UCS vs. cement content for 7 and 28 days of curing. Here, y is the UCS [MPa] and x is the time [days].

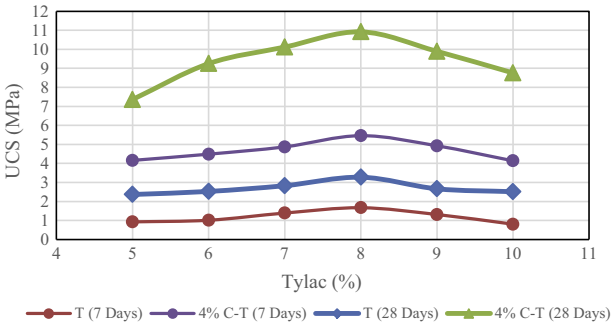

Fig. 5. Plot of UCS vs. Tylac® 4190 content. Here, "T" denotes Tylac® 4190.

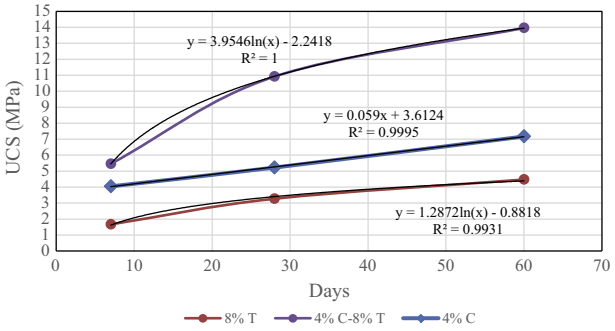

Fig. 6. Plot of UCS vs. curing time. Here, "C" denotes cement and "T" denotes Tylac® 4190; y is the UCS [MPa] and x is the time [days].

a concentration of 8%. However, after that, the UCS decreases on account of a higher water content of 44.92% of Tylac® 4190. The mechanism of this decrease has been explained in Section 5.1. Further, the results of UCS test reveal that it increase by 94.43%, upon the addition of a 4% Portland cement–8% Tylac® 4190 mixture relative to a specimen with only 4% cement.

Specifically, Fig. 6 shows the influence of curing time on the UCS via linear and nonlinear models. In this figure, it can be clearly seen that the UCS increases with an increase in the curing time, which indicates that the relative compressive strength obtained subsequent to curing for 7 days increases by about 77% after 28 days of curing and by 56% after 60 days of curing at a cement content of 4%.

5.3. Influence of cement content, water content, dry density, and Tylac® 4190 content on UCS

From Fig. 4, it is observed that the UCS increases linearly with the cement content and non-linearly with the dry density and Tylac® 4190 content as shown in Figs. 3 and 5 respectively. These results are in agreement with previous findings on the influence of cement content and dry density on cement-treated materials [36,37]. Xuan et al. [37] employed an adapted model to demonstrate the relationship between the UCS and the variables affecting it, i.e., the cement content, water content, and additive content:

$$f_c = K_1(C/W) \times (D)^{k_2} \times e^{k_3 \times M} \quad (1)$$

where f_c is the UCS [MPa]; K_1, K_2, and K_3 are adjustable variables; C is the cement content [%]; D is the dry density [g/cm^3]; W is the moisture content [%]; and M is the additive content [%].

Based on the experimental results, models for estimating the UCS of a mixture cured for 7 and 28 days are developed and expressed as follows:

$$f_c = 0.122(C/W) \times D^{4.857} \times e^{-0.001M}, \quad R^2 = 0.929 \quad (2)$$

$$f_c = 0.188(C/W) \times D^{4.997} \times e^{0.017M}, \quad R^2 = 0.928 \tag{3}$$

where M is the Tylac® 4190 content [%].

5.4. Influence of curing time

Curing time is another important factor affecting UCS. Fig. 6 shows the trend of UCS with a change in curing times at a cement content of 4%. It can be seen that the UCS increases almost linearly with increasing curing time. A number of studies have reported its influence on UCS [38–42]. For example, the relationship between UCS and curing time can be given as [43]

$$f_c(t) = f_c(t_0) + k_1 \times \log(t/t_0) \tag{4}$$

where $f_c(t)$ is the UCS at a curing age of t [days] and $f_c(t_0)$ is the UCS at a curing age of t_0 [days]. There exists another adapted prediction model that considers the influence of curing time on the UCS, which was proposed by Lim and Zollinger [44], as given in Eq. (5). This model is based on the calibration of the American Concrete Institute (ACI) Committee model, which introduces two adjustable variables (k_1 and k_2) for UCS estimation.

$$f_c(t) = f_c(28) \times \frac{t}{k_1 + k_2 \times t} \tag{5}$$

where $f_c(28)$ is the 28-day UCS. In this model, the relationship between the UCS and the curing time is expressed as in Eq. (6) using three adjustable variables (k_1, k_2, and k_3):

$$f_c(t) = k_1 \times k_2^{f_c(28)} \times t^{(k_3)} \tag{6}$$

Thus far, there are three models reported for RBS which consider the influence of curing time, such as the exponential model, the log-scale model, and the ACI model, expressed in Eqs. (7)–(9), respectively [37,44,45]:

$$f_c = k_1 \times (C/W) \times D^{k_2} \times e^{(k_3.M)} \times e^{[1-(28/t)^{k_4}]} \tag{7}$$

$$f_c = k_1 \times (C/W) \times D^{k_2} \times e^{(k_3.M)} \times [1 + k_4 log(t/28)] \tag{8}$$

$$f_c = k_1 \times (C/W) \times D^{k_2} \times e^{(k_3.M)} \times t/(5.1 + k_4 \times t) \tag{9}$$

Based on the experimental data derived from the present work, the above three estimation models are expressed as in Eqs. (10)–(12), respectively:

$$f_c = 0.197 \times (C/W) \times D^{4.972} \times e^{(0.014M)} \times e^{[1-(28/t)^{0.378}]}, \quad R^2 = 0.990 \tag{10}$$

$$f_c(t) = 0.197(C/W) \times D^{4.972} \times e^{0.014M} \times [1 + 0.828log(t/28)], \quad R^2 = 0.990 \tag{11}$$

$$f_c(t) = 0.108(C/W) \times D^{4.972} \times e^{0.014M} \times t/(5.1 + 0.368 \times t), \quad R^2 = 0.990 \tag{12}$$

5.5. ITS

The results of a test performed for determining the ITS are used to evaluate the relative quality of a mixture in conjunction with laboratory mix design testing and to estimate the possibility of rutting or cracking of the mixture. For this test, the mixture was prepared according to ASTM D 1632 and ASTM D 6926 using a metal cylindrical specimen mold with an internal diameter of 101.60 mm and height of 63.5 ± 2.5 mm. The average ITS of treated specimens cured for 7, 28, and 60 days was obtained using a hydraulic compressive strength testing machine. In accordance with ASTM D 6931, a vertical compressive ramp with a rate of 50 mm/min was applied until the maximum load was reached. The ITS is calculated as given in Eq. (13):

$$S_t = 2 \times P/\pi \times t \times D \tag{13}$$

where S_t is the ITS [MPa], P is the maximum load [N], t is the specimen height [mm], and D is the specimen diameter [mm]. The influences of the cement content, Tylac® 4190 content, and curing time on the ITS are shown in Figs. 7–9, respectively.

Specifically, Fig. 7 shows the influence of the cement content on the ITS for curing times of 7 days and 28 days, using two nonlinear models based on the experimental data. It can be seen that the ITS increases with increasing cement content.

Fig. 8 shows the influence of the Tylac® 4190 content on the ITS. It is seen that the tensile strength increases with increasing Tylac® 4190 content up to 8% and decreases after that because of the same mechanism as that described in Section 5.1, which also indicates that the optimum Tylac® 4190 content is 8%. The results of ITS test reveal that it increases by 90.45%, upon the addition of a 4% Portland cement–8% Tylac® 4190 mixture relative to a specimen with only 4% cement.

Eqs. (14) and (15) below represent the influence of the cement content, moisture content, dry density, and Tylac® 4190 content on the ITS.

$$S_t = 0.008(C/W) \times D^{5.458} \times e^{0.057M}, \quad R^2 = 0.957 \tag{14}$$

$$S_t = 0.074(C/W) \times D^{3.886} \times e^{0.013M}, \quad R^2 = 0.926 \tag{15}$$

Fig. 9 shows the influence of curing time on the ITS as determined using two linear models. The figure reveals that the ITS increases with increasing curing time, which indicates that curing time is an important factor in CTTB. Eqs. (16)–(18) below represent the influence of the cement content, moisture content, dry density, Tylac® 4190 content, and curing time on the ITS.

$$S_t(t) = 0.049 \times (C/W) \times D^{4.268} \times e^{(0.024M)} \times e^{[1-(28/t)^{0.309}]}, \quad R^2 = 0.974 \tag{16}$$

$$S_t(t) = 0.049(C/W) \times D^{4.268} \times e^{0.024M} \times [1 + 0.688log(t/28)], \quad R^2 = 0.974 \tag{17}$$

$$S_t(t) = 0.038(C/W) \times D^{4.268} \times e^{0.024M} \times t/(5.1 + 0.591 \times t), \quad R^2 = 0.974 \tag{18}$$

5.6. Resilient modulus of elasticity

The resilient modulus test can be used to evaluate the relative quality of materials for pavement design and analysis. Factors such as temperature, loading rate, rest periods, and frequencies are

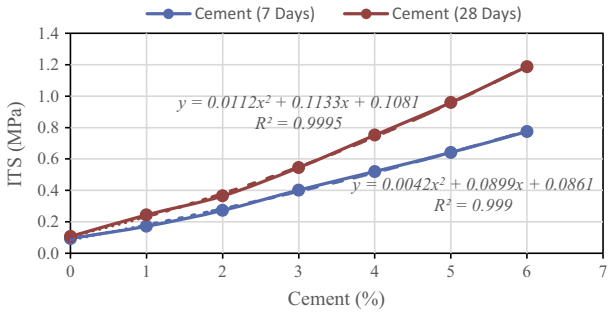

Fig. 7. Plot of ITS vs. cement content. Here, y is the ITS [MPa], and x is the time [days].

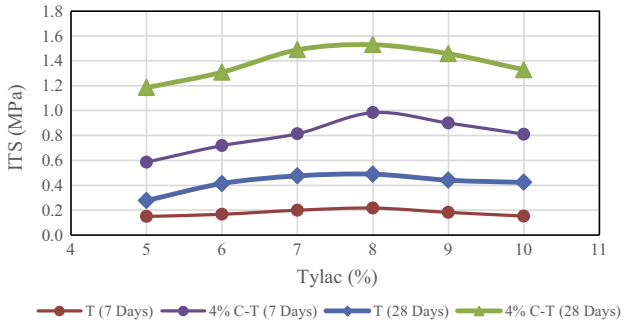

Fig. 8. Plot of ITS vs. Tylac® 4190 content. Here, "T" denotes Tylac® 4190.

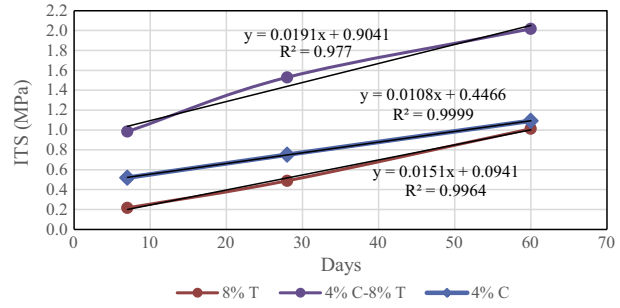

Fig. 9. Plot of ITS vs. curing time. Here, "C" denotes cement and "T" denotes Tylac® 4190; y is the ITS [MPa] and x is the time [days].

influential in this test method. In recent years, the philosophy of asphalt pavement design has undergone change from a more empirical approach to a mechanistic approach based on an elastic theory. Design methods based on the elastic theory require the elastic properties of pavement materials as input. The resilient modulus of a mixture, measured in the indirect tensile mode (ASTM D4123), is the most popular form of stress–strain measurement used to evaluate elastic properties [46,47].

The mixture for testing was prepared according to ASTM D 1632 and ASTM D 6926 using a metal cylindrical specimen mold with an internal diameter of 101.60 mm and height of 63.5 ± 2.5 mm. A repeated-load indirect tension test for determining the resilient modulus of each mixture was conducted according to ASTM D 4123 by applying compressive loads of 2000 N at 25 °C with a waveform at 1.0 Hz for loading frequencies (the recommended load range can be 10–50% of the ITS). The resulting horizontal deformation of a specimen with an assumed Poisson's ratio of 0.2 was measured, and five conditioning pulse counts were used to calculate the resilient modulus (ITRM). The values of horizontal deformation were measured using linear variable differential transducers (LVDTs). LVDTs should be positioned at mid-height opposite each other along the specimen's diameter. Each specimen was tested twice for measurement of the ITRM. Following the first test, the specimen was rotated by approximately 90°, and the test was repeated. The ITRM is calculated as given in Eq. (19):

$$E_{RT} = P(\upsilon_{RT} + 0.27) \times \Delta H_T \tag{19}$$

where E_{RT} is the resilient modulus of elasticity [MPa], P is the repeated load [N], υ_{RT} is the total resilient Poisson's ratio, and ΔH_T is the total recoverable horizontal deformation. The results of ITRM determination are shown in Figs. 10–12.

Specifically, Fig. 10 shows the influence of the cement content on the ITRM for curing times of 7 days and 28 days, determined using two linear models based on experimental data. It can be seen that the ITRM increases with an increase in cement content.

Fig. 11 shows the influence of the Tylac® 4190 content on the ITRM. In accord with the mechanism described in Section 5.1, in Fig. 11, it is seen that the ITRM increases with increasing Tylac® 4190 content up to 8% and it decreases after that; this indicates that the optimum Tylac® 4190 content is 8%. The results of ITRM test reveal that it increases by 45.41%, upon the addition of a 4% Portland cement–8% Tylac® 4190 mixture relative to a specimen with only 4% cement.

Eqs. (20) and (21) below represent the influence of the cement content, moisture content, dry density, and Tylac® 4190 content on the ITRM.

$$E_{RT} = 0.161(C/W) \times D^{5.420} \times e^{0.010M}, \quad R^2 = 0.950 \tag{20}$$

$$E_{RT} = 2.003(C/W) \times D^{3.394} \times e^{(-0.004M)}, \quad R^2 = 0.958 \tag{21}$$

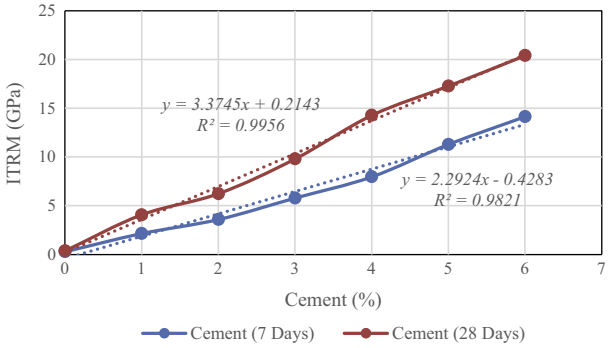

Fig. 10. Plot of ITRM vs. cement content. Here, y is the ITRM [GPa] and x is the cement content [%].

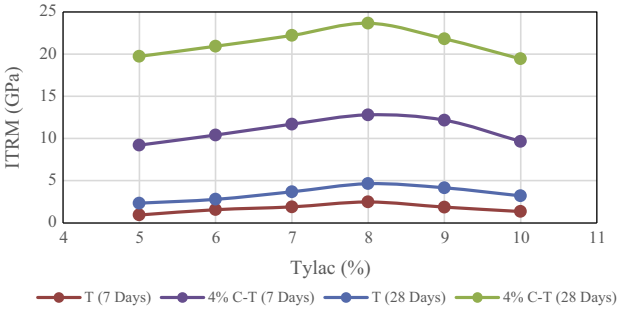

Fig. 11. Plot of ITRM vs. Tylac® 4190 content. Here, "C" denotes cement and "T" denotes Tylac® 4190.

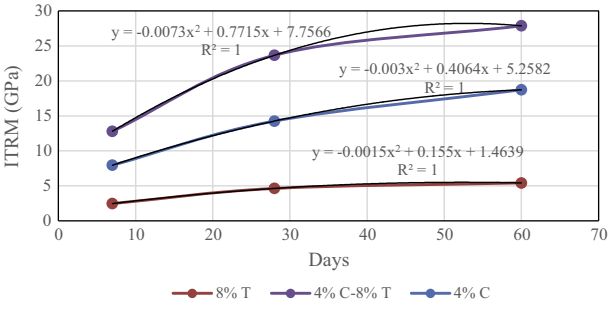

Fig. 12. Plot of ITRM vs. curing time. Here, "C" denotes cement and "T" denotes Tylac® 4190; y is the ITRM [GPa] and x is the curing time [days].

Fig. 12 shows the influence of the curing time on the ITRM as determined using nonlinear models. The ITRM is seen to increase with an increase in curing time, which indicates that curing time is an important factor in CTTB. Eqs. (22)–(24) below represent the influence of cement content, moisture content, dry density, Tylac® 4190 content, and curing time on the ITRM.

$$E_{RT} = 1.355 \times (C/W) \times D^{3.821} \times e^{(-0.001M)} \times e^{[1-(28/t)^{0.366}]}, \quad R^2 = 0.974 \tag{22}$$

$$E_{RT}(t) = 1.355(C/W) \times D^{3.821} \times e^{(-0.001M)} \times [1 + 0.803log(t/28)], \quad R^2 = 0.992 \tag{23}$$

$$E_{RT}(t) = 0.792(C/W) \times D^{3.821} \times e^{(-0.001M)} \times t/(5.1 + 0.402 \times t), \quad R^2 = 0.992 \tag{24}$$

5.7. Wetting and drying

ASTM D 559 prescribes steps for determining volume changes (swell and shrinkage), water content changes, and soil aggregate–cement losses, all induced by subjecting hardened soil aggregate–cement specimens to 12 WD cycles. The specimens were compacted into a cylindrical metal mold with a capacity of 944 cm^3 and internal diameter of 101.6 mm using the compaction procedure described in Section 5.1 according to ASTM D 558. The specimens were placed in the moist room, and they were protected from free water for 7 days. They were then weighed and measured at the end of the curing period to prepare data for evaluating their water content and volume. Then, the specimens were submerged in potable water at room temperature for 5 h and then removed. Subsequently, the specimens were weighed and measured again in terms of their volume and moisture changes. Then, they were placed in an oven at 71 °C for 42 h, following which they were removed, weighed, and measured. They were next provided two firm strokes on their sides and at each end with a wire scratch brush (20 brush strokes for sides and 4 strokes for each end). The specimens were then submerged in water, and this process was repeated for 12 cycles. The volume change was calculated as a percentage of the subsequent volumes of the specimens and the original volumes of the specimens at the time of molding. Both the water content of a specimen at the time of molding and the subsequent water content as a percentage of the original oven-dry weight of the specimens were calculated. The soil aggregate–cement loss was calculated as a percentage of the final oven-dry weight and the original oven-dry weight of the specimens. The results of the WD test are shown in Figs. 13–17.

Figs. 13–15 show the results of soil aggregate–cement losses, water content changes, and volume changes for 4% cement, 8% Tylac® 4190, and a mixture of 4% cement and 8% Tylac® 4190, induced by subjecting hardened soil aggregate–cement specimens to 12 WD cycles with the aim of determining the resistance of compacted soil aggregate–cement specimens to repeated WD. From the figures, it is clear that the average water absorptions of 4% cement, 8% Tylac® 4190, and 4% cement–8% Tylac® 4190 mixture are 4.842%, 0.960%, and 0.630%, respectively, for each WD cycle. This result indicates that use of the 4% cement–8% Tylac® 4190 mixture reduces the water absorption in each cycle by 86.99% compared to the use of only cement in the mixture. Further, the average volume changes of 4% cement, 8% Tylac® 4190, and 4% cement–8% Tylac® 4190 mixture are 0.572%, 0.159%, and 0.065%, respectively, for each WD cycle. This result indicates that use of the 4% cement–8% Tylac® 4190 mixture reduces the volume change in each cycle by 83.17% compared to the use of only cement in the mixture. Finally, it is seen from the figures that the average

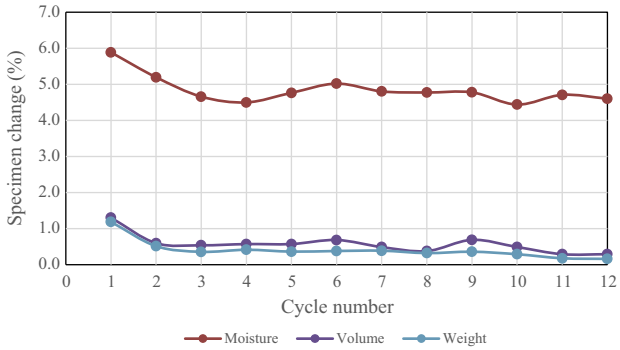

Fig. 13. Moisture, volume, and weight changes of cement over 12 WD cycles.

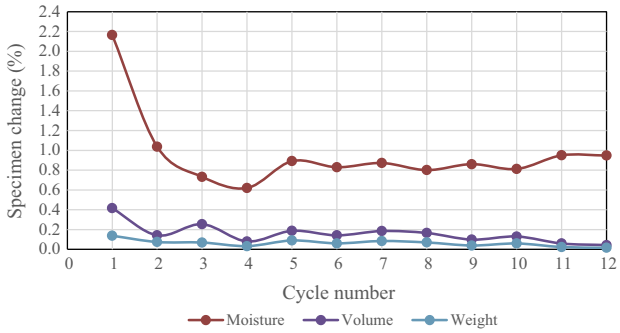

Fig. 14. Moisture, volume, and weight changes of Tylac® 4190 over 12 WD cycles.

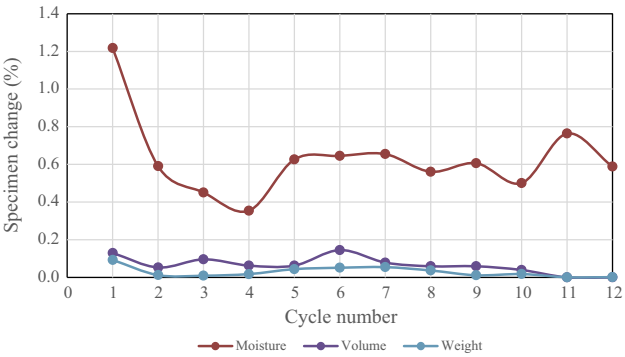

Fig. 15. Moisture, volume, and weight changes of cement–Tylac® 4190 mixture over 12 WD cycles.

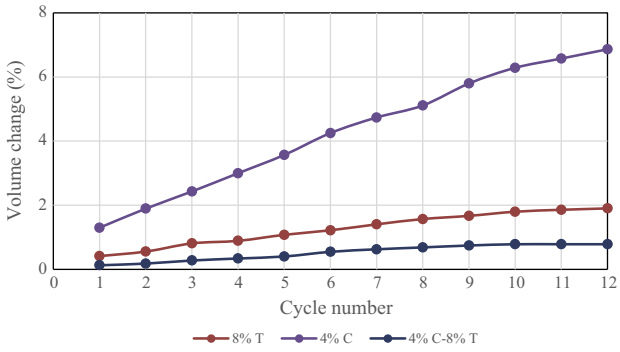

Fig. 16. Total volume change over 12 WD cycles. Here, "C" denotes cement and "T" denotes Tylac® 4190.

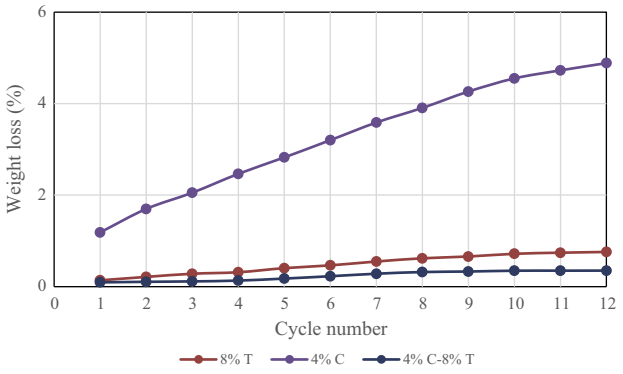

Fig. 17. Total weight loss over 12 WD cycles. Here, "C" denotes cement and "T" denotes Tylac® 4190.

weight changes of 4% cement, 8% Tylac® 4190, and 4% cement–8% Tylac® 4190 mixture are 0.407%, 0.063%, and 0.029%, respectively, for each WD cycle. This result indicates that use of the 4% cement–8% Tylac® 4190 mixture reduces the weight change in each cycle by 92.83% compared to the use of only cement in the mixture. It should be noted that the soil-aggregate sample without any additive failed in cycle 1 because of 100% water absorption, 100% volume change, and 100% weight loss.

Figs. 16 and 17 show the results of the total volume change and total soil aggregate–cement losses for 4% cement, 8% Tylac® 4190, and a 4% cement–8% Tylac® 4190 mixture induced by subjecting hardened soil aggregate–cement specimens to 12 WD cycles. It is seen that the total volume changes of cement, Tylac® 4190, and the cement–Tylac® 4190 mixture are 6.863%, 1.903%, and 0.786%, respectively, after 12 WD cycles. Further, the total weight changes of cement, Tylac® 4190, and the cement–Tylac® 4190 mixture are found to be 4.885%, 0.758%, and 0.350%, respectively, after 12 WD cycles. The results of the test conducted to determine the resistance of the specimens to WD cycling (durability) show that the addition of the 4% Portland cement–8% Tylac® 4190 mixture resulted in reductions of 86.99% in both water absorption and permeability, volume changes of 88.55%, and weight changes of 92.84% relative to a specimen with only 4% cement after 12 WD cycles.

6. Conclusion and recommendation

The effects of moisture content, dry density, cement content, Tylac® 4190 content, and curing time on the strength of road base materials were investigated via WD cycle tests as long-term performance and UCS, ITS, and ITRM in order to evaluate the short-term performances of CTB and CTTB mixture. The strength of the road base layer was found to increase with increasing cement content and longer curing time. It should be noted that while selecting an optimum content of Portland cement, it is not cost effective to choose the highest percentage of cement; furthermore, using an excessive amount of cement causes shrinkage cracks, which are a severe problem for pavements because they lead to water infiltration. The results of our tests show that the strength increases with an increase in the Tylac® 4190 content up to 8%, after which it decreases. This might be due to the water content (44.92%) of Tylac® 4190 causes a reduction in the dry density and strength of the mixture. The test results showed that application of CTTB to soil-aggregate is an effective treatment for effectively improving its strength, reducing water vulnerability, and increasing the bearing capacity of the pavement. All these strength and durability improvements result in a significant increase in the lifetime of the pavement. In addition, the total number of roadway layers in CTTB is lesser than those in the conventional variant because of higher bearing capacity, which effectively reduces the construction time and cost. Results of the WD tests show that Portland cement and Tylac® 4190 can improve the resistance of CTTB mixtures to moisture damage and reduce both soil aggregate–cement losses and volume changes (swell and shrinkage). This implies that introducing Portland cement and Tylac® 4190 into soil-aggregate mixtures reduces their moisture susceptibility because both these components are effective adhesive agents for mixtures.

On the basis of the analysis of the results of this study, the following conclusions and recommendations are made:

1. CTTB has good mechanical properties as road base. The study results indicate that CTTB produces a good cemented road base with a high load-spreading capacity.
2. On the basis of the study findings, the optimum contents of cement and Tylac® 4190 in the pavement base layer are recommended as being 4% and 8%, respectively.
3. The results show that the addition of Portland cement and Tylac® 4190 increases the compressive strength, pH, resilient modulus, and tensile strength of the mixture.
4. The results of UCS, ITS, and ITRM tests reveal that they increase by 94.43%, 90.45%, and 45.41%, respectively, upon the addition of a 4% Portland cement–8% Tylac® 4190 mixture relative to a specimen with only 4% cement.
5. The results of a test for determining the resistance of specimens to WD cycling (durability) show that the addition of the 4% Portland cement–8% Tylac® 4190 mixture resulted in reductions of 86.99% in both water absorption and permeability, volume changes of 88.55%, and weight changes of 92.84% relative to a specimen with only 4% cement after 12 WD cycles.
6. An estimation model each for the UCS, ITS, and ITRM of CTTB was developed in terms of mixture variables such as the cement content, water content, dry density, Tylac® 4190 content, and curing time.
7. It is recommended that in practice, other structural properties of CTTB should also be considered for optimum mixture design. Other structural properties of great importance include flexural strength (modulus of rupture), creep (permanent deformation) behavior, and the chemical reaction properties.

Acknowledgements

The authors would like to thank the Sustainable Urban Transport Research Centre (SUTRA) at the Faculty of Engineering and Built Environment of Universiti Kebangsaan Malaysia (UKM) and Mallard Creek Polymers, Inc. (MCP) for providing research materials and facilities. The authors also acknowledge the Ministry of Science, Technology and Innovation (MOSTI) of Malaysia for the research funding provided through Project 03-01-02-SF0999. Finally, the authors are grateful to the University of Malaya (UM) for experimental collaboration.

References

[1] Goodary R, Lecomte-Nana GL, Petit C, Smith DS. Investigation of the strength development in cement-stabilised soils of volcanic origin. Construct Build Mater 2012;28(1):592–8.
[2] Al-Amoudi OSB, Khan K, Al-Kahtani NS. Stabilization of a Saudi calcareous marl soil. Construct Build Mater 2010;24(10):1848–54.
[3] Basha EA, Hashim R, Mahmud HB, Muntohar AS. Stabilization of residual soil with rice husk ash and cement. Construct Build Mater 2005;19(6):448–53.
[4] Horpibulsuk S, Rachan R, Chinkulkijniwat A, Raksachon Y, Suddeepong A. Analysis of strength development in cement-stabilized silty clay from microstructural considerations. Construct Build Mater 2010;24(10):2011–21.
[5] Maslehuddin M, Al-Amoudi OSB, Shameem M, Rehman MK, Ibrahim M. Usage of cement kiln dust in cement products – research review and preliminary investigations. Construct Build Mater 2008;22(12):2369–75.

[6] Sariosseiri F, Muhunthan B. Effect of cement treatment on geotechnical properties of some Washington State soils. Eng Geol 2009;104(1):119–25.
[7] Van Gemert D, Czarnecki L, Maultzsch M, Schorn H, Beeldens A, Łukowski P, et al. Cement concrete and concrete–polymer composites: two merging worlds. Cem Concr Compos 2005;27(9–10):926–33.
[8] Fowler DW. Polymers in concrete: a vision for the 21st century. Cem Concr Compos 1999;21(5–6):449–52.
[9] Ohama Y. Principle of latex modification and some typical properties of latex-modified mortars and concretes adhesion; binders (materials); bond (paste to aggregate); carbonation; chlorides; curing; diffusion. ACI Mater J 1987;84(6):511–8.
[10] Yang Z, Shi X, Creighton AT, Peterson MM. Effect of styrene–butadiene rubber latex on the chloride permeability and microstructure of Portland cement mortar. Construct Build Mater 2009;23(6):2283–90.
[11] Ma H, Li Z. Microstructures and mechanical properties of polymer modified mortars under distinct mechanisms. Construct Build Mater 2013;47:579–87.
[12] Shaker FA, El-Dieb AS, Reda MM. Durability of styrene–butadiene latex modified concrete. Cem Concr Res 1997;27(5):711–20.
[13] Monteny J, De Belie N, Vincke E, Verstraete W, Taerwe L. Chemical and microbiological tests to simulate sulfuric acid corrosion of polymer-modified concrete. Cem Concr Res 2001;31(9):1359–65.
[14] Pacheco-Torgal F, Jalali S. Sulphuric acid resistance of plain, polymer modified, and fly ash cement concretes. Construct Build Mater 2009;23(12):3485–91.
[15] Li G, Zhao X, Rong C, Wang Z. Properties of polymer modified steel fiber-reinforced cement concretes. Construct Build Mater 2010;24(7):1201–6.
[16] Wang R, Wang P-M. Formation of hydrates of calcium aluminates in cement pastes with different dosages of SBR powder. Construct Build Mater 2011;25(2):736–41.
[17] Barluenga G, Hernández-Olivares F. SBR latex modified mortar rheology and mechanical behaviour. Cem Concr Res 2004;34(3):527–35.
[18] Wang R, Wang P-M, Li X-G. Physical and mechanical properties of styrene–butadiene rubber emulsion modified cement mortars. Cem Concr Res 2005;35(5):900–6.
[19] Rossignolo JA, Agnesini MVC. Durability of polymer-modified lightweight aggregate concrete. Cem Concr Compos 2004;26(4):375–80.
[20] Ohama Y. Polymer-based materials for repair and improved durability: Japanese experience. Construct Build Mater 1996;10(1):77–82.
[21] Garber S, Rasmussen RO, Harrington D. Guide to cement-based integrated pavement solutions. Institute for Transportation, Portland Cement Association: Iowa State University, US; 2011.
[22] Shojaei Baghini M, Ismail A, Kheradmand B, Hafezi MH, Alezzi Almansob R. Bitumen-cement stabilized layer in pavement construction using indirect tensile strength (ITS) method. Res J Appl Sci, Eng Technol 2013;5(24):5652–6.
[23] Freeme CR, Maree JH, Viljoen AW. Mechanistic design of asphalt pavements and verification using the heavy vehicle simulator. Pretoria, South Africa: Nat Inst Transp Road Res 1982;25:64–6.
[24] Xuan D. Literature review of research project: structural properties of cement treated materials. Section Road and Railway Engineering: Delft University of Technology, Netherland; 2009.
[25] Bell F. Engineering treatment of soils. London: E & FN Spon: Taylor & Francis; 2002.
[26] Eren Ş, Filiz M. Comparing the conventional soil stabilization methods to the consolid system used as an alternative admixture matter in Isparta Darıdere material. Construct Build Mater 2009;23(7):2473–80.
[27] Pérez P, Agrela F, Herrador R, Ordoñez J. Application of cement-treated recycled materials in the construction of a section of road in Malaga, Spain. Construct Build Mater 2013;44:593–9.
[28] NITRR. Cementitious Stabilizers in Road Construction: National Institute for Transport and Road Research, South Africa. Highway Materials Committee, Committee of State Road Authorities; 1986.
[29] PCA. Soil-cement laboratory handbook (ASTM/AASHTO Soil-Cement Testing procedures). Kokie (IL), US: Portland Cement Association; 1992.
[30] ACI C. State-of-the-art report on soil-cement. ACI Mater J 1990;87(4):395–417.
[31] ASTM. American Society for Testing and Materials (ASTM). West Conshohocken (PA), USA; 2004.
[32] ACI. State-of-the-art report on soil cement. Detroit, USA: American Concrete Institute; 1997.
[33] ARMY. Soil stabilization for pavements. TM 5-822-14. Washington, DC: Department of the Army, the Navy and the Air Force; 1994.
[34] Jones D, Jones D. Guidelines for the Stabilization of Subgrade Soils in California. California: UCD-ITS-RR-10-38, Institute of Transportation Studies, University of California, Davis; 2010.
[35] Lade PV, Liggio C, Yamamuro JA. Effects of non-plastic fines on minimum and maximum void ratios of sand. ASTM Geotech Test J 1998;21(4):336–47.
[36] Xuan DX, Houben LJM, Molenaar AAA, Shui ZH. Mechanical properties of cement-treated aggregate material – a review. Mater Des 2012;33:496–502.
[37] Xuan D, Molenaar AA, Houben LJ. Compressive and indirect tensile strengths of cement-treated mix granulates with recycled masonry and concrete aggregates. J Mater Civil Eng 2011;24(5):577–85.
[38] Tingle JS, Newman JK, Larson SL, Weiss CA, Rushing JF. Stabilization mechanisms of nontraditional additives. Transp Res Rec: J Transp Res Board 2007;1989(1):59–67.
[39] Molenaar A. Design of flexible pavement, lecture note CT 4860 structural pavement design. The Netherlands: Delft University of Technology; 2007.
[40] Shojaei Baghini M, Ismail A, Kheradmand B, Hafezi MH, Alezzi Almansob R. The potentials of Portland cement and bitumen emulsion mixture on soil stabilization in road base construction. J Teknol 2013;65(2):67–72.
[41] Sherwood PT. Soil stabilization with cement and lime. Department of Transport, London: Transport Research Laboratory; 1993.
[42] Hazirbaba K, Gullu H. California Bearing Ratio improvement and freeze–thaw performance of fine-grained soils treated with geofiber and synthetic fluid. Cold Reg Sci Technol 2010;63(1–2):50–60.
[43] Maher A, Szalaj WM, Bennert T. Evaluation of Poisson's Ratio for Use in the Mechanistic Empirical Pavement Design Guide (MEPDG). Division of Research and Technology, Rutgers University. Center for Advanced Infrastructure & Transportation, United States. Federal Highway Administration: Department of Transportation; 2008.
[44] Lim S, Zollinger DG. Estimation of the compressive strength and modulus of elasticity of cement-treated aggregate base materials. Transp Res Rec: J Transp Res Board 2003;1837(1):30–8.
[45] Terrel RL, Epps JA, Barenberg E, Mitchell J, Thompson M. Soil stabilization in pavement structures, a user's manual, Pavement design and construction considerations, vol. 1. Washington DC: Federal Highway Administration, Department of Transportation; 1979.
[46] Tayfur S, Ozen H, Aksoy A. Investigation of rutting performance of asphalt mixtures containing polymer modifiers. Construct Build Mater 2007;21(2):328–37.
[47] Niazi Y, Jalili M. Effect of Portland cement and lime additives on properties of cold in-place recycled mixtures with asphalt emulsion. Construct Build Mater 2009;23(3):1338–43.